euspen's 23rd International Conference & Exhibition, Copenhagen, DK, June 2023

www.euspen.eu

Fabrication and metrology of primary mirror in a 250-mm aperture three-mirror-anastigmat

Matthew A. Davies[1,2], Brian S. Dutterer[1], Aaron Bauer[3], Lucas Ochs[1], Glenn Boreman[1], Jannick P. Rolland[3]

[1]*The University of North Carolina at Charlotte, Charlotte, NC, 28223*
[2]*Moore Nanotechnology Systems, 6510 Northpark Blvd, Charlotte, NC, 28216*
[3]*The Institute of Optics, The University of Rochester, Rochester NY, 14627*

matt.davies@nanotechsys.com

Abstract

Freeform optics allow infinite optical design degrees of freedom which can be used to simplify traditional optical designs (reduced size, weight, and number of components) while maintaining or even improving optical performance. However, while optical designs may be simplified, complications arise in manufacturing, metrology and opto-mechanical design that necessitate a concurrent engineering. The target system is a 250-mm aperture freeform three mirror anastigmat imager operating at F/3 over a 2.12° by 2.12° full field of view prototyped in aluminum 6061 T6. Two of the most challenging aspects of the work are the manufacturing and opto-mechanical mounting of the freeform mirrors in the system to the tolerances required for detector limited performance. The methodology for achieving these tolerances and results are reported for a 190 mm freeform mirror. On-machine metrology is done with a linear variable differential transformer (LVDT) integrated with the machine controller. The freeform mirror is machined to near net shape on a precision machining center. It is then mounted kinematically to an ultraprecision diamond turning machine and its initial form is measured. The kinematic mount's repeatability is assessed by repeated unmounting, mounting and measurement with the LVDT probe to find the six degrees of freedom for the mirror position. A semi-finish cut of the freeform shape is made with a carbide tool, and the form is measured. The mirror is finished with a single crystal diamond tool, corrected and measured two more times. The final demonstrated peak to valley form error is 420 nm and the final uncertainties for the system met the goals.

Freeform optics, Ultraprecision diamond machining, Three-mirror anastigmat

1. Introduction

Freeform optics, containing optical surfaces with no axis of rotational invariance (within or beyond the optical part), introduce additional optical design degrees of freedom with potentially radical system improvements [1]. These include reduced size and weight, improved performance, reduced system cost, improved manufacturability, and often entirely new optical functionality [2,3]. For imaging and surveillance, wide field of view, large aperture, and unobstructed systems with optimization of aberrations over the full field of view are possible using freeform systems. However, a judicious choice of the starting geometry in the optical design is critical to maintaining feasibility and control costs [4,5]. Further, realizing the benefits of freeform optics in the final physical imaging systems requires a concurrent engineering approach where optical design, fabrication, metrology, opto-mechanics, and desired field performance are considered simultaneously [6,7]. The design presented here is a variation of a one-third scale imager that was demonstrated previously [8].

2. Optical and Opto-mechanical Design

A freeform imager of this size is characterized by a number of challenges: (1) an optimized optical design; (2) coordination between the optical design and the opto-mechanical design to ensure that tolerances can be met with existing equipment, that is suited for manufacturing, metrology and meeting of the form and rigid body placement tolerances; (3) manufacturing and correction of mirror form to meet tolerances; (4) validation of

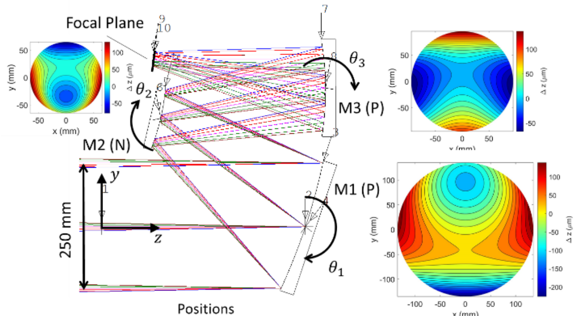

Positions

Element	x (mm)	y (mm)	z (mm)	θ, (deg)
M1	0.000000000	0.000000000	400.000000000	18.395373000
M2	0.000000000	213.757558200	115.602574020	13.159266000
M3	0.000000000	273.719981160	439.640849220	-0.451869200
Focal Plane	0.000000000	331.255053940	100.046206064	7.615899600

Figure 1. Optical design and ray-trace diagram for freeform TMA (significant figures as provided by CODE V software.)

the placement accuracy and ease of assembly in the opto-mechanical design.

2.1. Optical Design

The optical design is shown in Figure 1. The mirrors are freeform with a base asphere. The system is a 250 mm aperture-class three-mirror imager operating at F/3 over a 2.12° by 2.12° full FOV, with diffraction-limited performance (optical design) across the FOV in the visible spectrum. The optical system volume is 40 L, with a detector measuring 36.4 mm by 27.6 mm with 4.6 µm pixel pitch. Although it is a freeform design, the dominant base aspheres in the design are positive-negative-

Table 1. Tolerances for detector limited performance.

Detector Limited Performance			
Motion	M1	M2	M3
X/Y Decenter [µm]	±125	Compensator	±125
Z Despace [µm]	±125	Compensator	±125
Tip/Tilt [µrad]	±115	±115	±115
Clocking [µrad]	±475	±475	±475
Irregularity (PV) [µm]	2 (1)	0.92 (0.46)	1.41 (0.71)
Power (Fringes*)	5	5	5

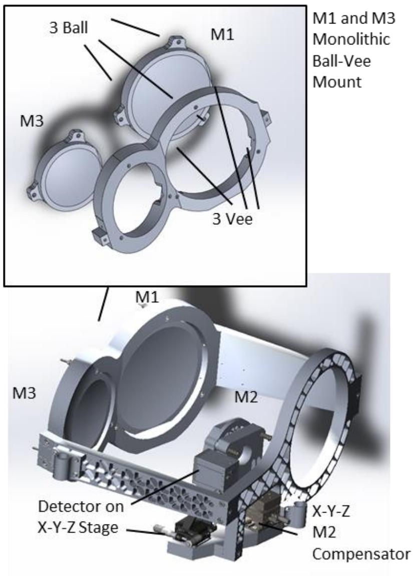

Figure 2. Full scale freeform TMA design.

positive (PNP). The topographical layout of the system is important for performance optimization (see Bauer et al. [5]).

2.2. Previous Opto-Mechanical Design

A third scale version of a similar system is described in Horvath et al. [8]. Lessons learned from this system were integrated into the design of the full-scale system described here. The third-scale system incorporated a fully monolithic frame and three-ball three-vee kinematic mounts to achieve a "snap-together" design that could be disassembled and assembled and be imaging in less than 15 minutes. However, because the system did not allow for any adjustment of mirror positions, the tolerances required to achieve detector limited performance were very difficult to attain. The kinematic balls on the freeform mirrors were diamond milled in the same set-up as the cutting of the freeform optical surfaces. The final system did not achieve detector limited performance, but did produce some encouraging results. First, though it imaged, wavefront error was 1.25 µm, far worse than detector limited performance. But the RMS wavefront repeatability upon assembly and disassembly was 25 nm, indicating that the snap-together kinematic design was very repeatable. It is likely that there were significant form errors in the mirrors. At the time, these could not be measured. It is also likely that the mirror placements did not meet sub-micrometer tolerances because the vee-grooves in the housing were not re-machined on the ultraprecision machining system. Finally, no performance recovery adjustments were possible. The optomechanical design for the larger system addressed these potential problems by maintaining the snap-together ball-vee mounts but allowing adjustment of one mirror (M2) to recovery performance.

2.3. Full Scale Opto-Mechanical Design

The final opto-mechanical design is shown in Figure 2. Based on experience with the prototype, three linear degrees of adjustment were added to mirror M2 using a commercially available precision stage. This allowed detector limited performance to be achieved with the tolerances shown in Table 1. Two tolerances are given for the mirror form. The number in parentheses is the allowed PV form error. The black number is the allowable form error if it is only astigmatism and power. The red number is for error containing other Zernike terms. The freeform deviation of the mirrors is dominated by astigmatism and thus the machine tracking errors dominated by astigmatism thus, the important of this tolerance. By using a concurrent approach, it was possible to use the freeform optical design and the minimum performance recovery degrees of freedom on M2 to maintain a nearly snap together design. The placement tolerances were loose enough that housing components were machinable on a conventional precision machine (Makino A51). Form tolerances on the mirrors required the were similarly expanded to be achievable on the higher performance Moore Nanotechnology 650 FG by coordinated axis diamond turning (sloe-slide servo). The goal is optimized for manufacturability at reasonable cost.

2.4. Methodology for Manufacturing and Error Correction

Mirror M3 is the focus of this paper. The clear aperture is 184 mm, the saggital depth is approximately 7.7971 mm, and the deviation from the base asphere (freeform deviation) is 213.456 µm. The form tolerance target is 710 nm peak-to-valley (PV). To accomplish this, the following experimental metrology was employed.

1. Mill the lightweight structure and spheres on the back of each mirror on a Makino A51.
2. Mount mirror with the 10 mm spheres on the precision machining center with three-vee base and mill the near net shape freeform and the spheres on the front of the mirror.
3. Center and align a vee-mounting fixture on the Moore Nanotechnology 650FG with on-machine LVDT.
4. Mount mirror on vee-mount on the Moore Nanotechnology 650FG. and measure with LVDT.
5. Semi-finish machine freeform surface with a carbide tool.
6. Finish machine freeform surface with a diamond tool and measure with LVDT, and fit errors to Zernike polynomials.
7. Machine final surface with diamond tool.

While manufacturing the mirror, it was also required to use on-machine metrology to estimate assembly tolerances as well.

3. Mirror Surface Finishing, Metrology and Correction

A Moore Nanotechnology 650FG with five axes (X-Y-Z-B-C) was used to diamond turn and measure the mirror surfaces, assess the mount position uncertainty, and correct the surfaces. While independent metrology is preferred, time and equipment constraints have precluded it thus far.

3.1. Mirror Prescriptions

The mirror prescriptions were given by the sum of a leading aspheric term and fringe Zernike polynomials.

$$z(\rho,\phi) = \frac{\rho^2}{R\left(1+\sqrt{1-(1+\kappa)\left(\frac{\rho^2}{R^2}\right)}\right)} + \sum_n Z_n(r,\phi) \quad (1)$$

The equation describes the surface height z in polar coordinates, radial distance from center, ρ, and angle, ϕ, measured with the right-hand rule about z. The term r is the normalized radius ρ/R_{norm} where R_{norm} is the normalizaiton radius. The terms R and κ are the base radius of curvature and conic constant of the axisymmetric aspheric term. The Zernike terms Z_1, Z_2, Z_3, etc., are the standard Fringe Zernike polynomials piston, x-tilt, y-tilt, etc. M3 has been discussed. M1 and M2 have clear apertures of 260 mm and 130 mm, respectively. The saggital depths are 7.9336 mm, 5.3438 mm, respectively, and the freeform deviations are 156.732 μm and 220.419 μm, respectively.

3.2. Mirror Machining

The mirrors were diamond machined with coordinated axis diamond turning on the Nanotech 650FG (Figure 3(a) and 3(e)) programmed with NanoCAM4. This required both precision machine mounting (3 sphere/3 vee) that matched the housing mount design, form and finish generation by diamond turning, and on-machine metrology. Figure 3(b) shows the three spheres on mirror M2 mating with the three vees on the machine mounting fixture. When a mirror was mounted on the machine, the three-vee fixture was mounted first with the inner bolt circle of twelve 10-32 screws shown in Figure 3(c). The screws were initially tightened with a moment of 56.5 N-cm. Next precision ground cylinder artefacts with the same radius (10.0 mm) as the mounting spheres were lightly greased and mounted with 56.5 N-cm of moment with two self-aligning spherical washers. The on-machine LVDT (Figure 3(d)) was used to measure the heights of the artefacts and the inner screw moments were adjusted so that the artefact peaks were co-planar. For mirror M3, with a nominal height set to zero, the artefacts were levelled so that $\bar{z}_0 = 32.8\,\mathrm{nm} \pm 87\,\mathrm{nm}$, $\bar{z}_{120} = 146.4 \pm 106.8\,\mathrm{nm}$, $\bar{z}_{240} = 148.4 \pm 99.2\,\mathrm{nm}$ (Figure 3(c)). The large uncertainties are due to repeated measurements along 0.5 mm of the artefact crests and are mainly due to surface roughness. Mirror tilt due to these height differences are on the order of 1 μrad, much less than the 250 μrad tolerances in Table 1. By writing a custom routine to measure the balls on the front of the mirror (Figure 3(f) inset), which are used to mount the system in the final assembly, mirror mounting uncertainty in 6 degrees of freedom was determined. While the details of that analysis cannot be detailed in this paper, the results of repeated mount/remount of mirror M3 on the machine spindle using the vee-mount were an x/y decenter of ±3 μm, z-despace of ±7, tip/tilt of ±4 μrad, and clocking of ±2 μrad. These also reflect the assembly uncertainties in the final system and are significantly lower than the overall tolerance goals in Table 1.

The mirror blanks were first milled on the A51 using code from NanoCAM4, and then turned to near net shape using X-Z-C turning. The tool cut from the outer diameter to the mirror center while the mirror rotated counter clockwise (negative C) as shown in Figure 3(f) and Figure 4 (a). The tools had 0.5 mm nominal diameter, zero-rake angle and waviness controlled below 100 nm. The mean rate of rotative was 83 rpm. The feed per revolution was 6 μm and the surface roughness was near the theoretical Sa of 2.3 nm.

3.3. Mirror Metrology

The LVDT probe on the machine has 18 nm resolution. The repeatability of a measurement at any single point has a standard deviation of less than 25 nm. If the standard deviation is found to exceed 25 nm, the pressure, tip tightness, etc., are adjusted to recover the repeatability. The LVDT is triggered in the machine controller when it contacts the surface, and machine positions can be recorded at each trigger position. It was not only used to measure the fixture heights and ball locations as discussed in the previous section, but was used to measure mirror form and surface location relative to the mounting spheres. The measurement arrangement is shown in Figure 4. Mirrors M1 and M3 were too large for the machine Y travel to reach every point, so a polar pattern was used as shown in Figure 3. The prescription coordinates x, y and $z(\rho,\phi)$ are shown in Figure 3 (a) (black) and the machine motion coordinates X, Y, and C are shown in blue. However, for other spherical and freeform specimens Cartesian and polar probing patterns have been compared. To avoid replication of axis errors from cutting into measurement, the mirror was cut and measured in the opposite directions as shown in Figure 4.

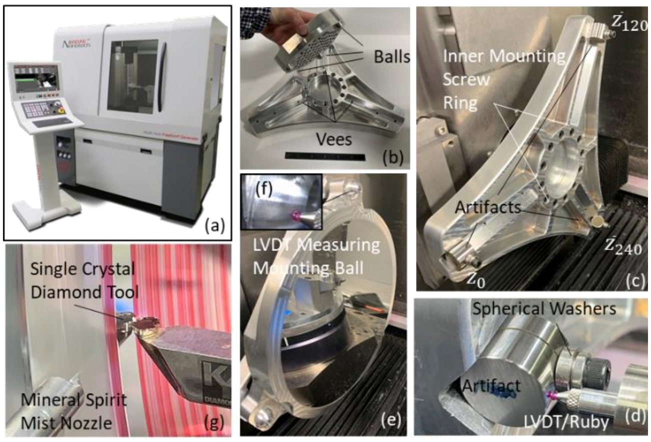

Figure 3. Diamond machining of mirror surfaces.

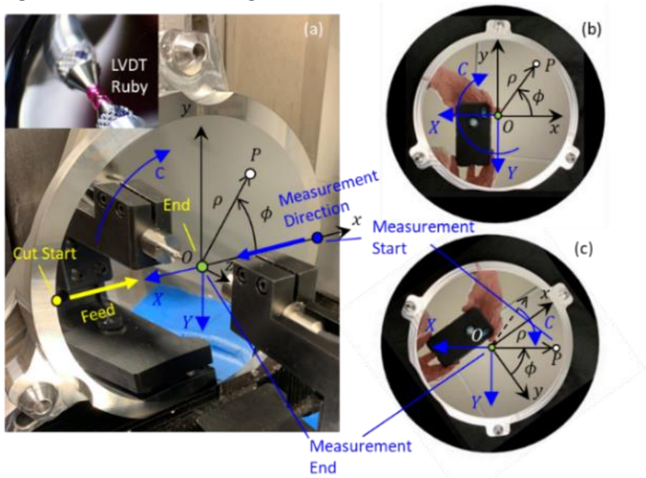

Figure 4. Diamond machining of mirror surfaces.

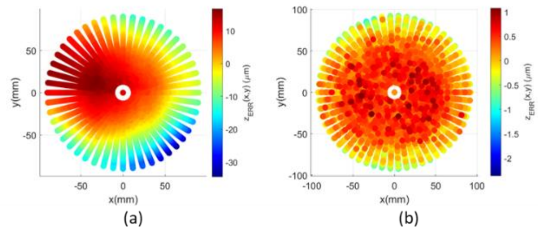

Figure 5. (a) Near net mirror on three-vee mount, (b) measured error, (c) mirror being semi-finished with carbide tool, (d) measured error.

A custom code was developed in MATLAB® to begin with the analytical mirror prescriptions and generate an NC code to do the measurements and process the measured data. To probe the radial line $\overline{OP}$ in Figure 4(a) and 4(b), the machine C axis is rotated by nominal angle ϕ clockwise (Figure 4(c)), and the machine X axis is used to move the probe to discrete points along ρ. Locating the ball center position for each surface point required evaluation of the local surface normal vector with components n_ρ, n_ϕ and n_z. On an asphere, $n_\phi = 0$, so no lateral adjustment of position is needed. On a freeform, $n_\phi \neq 0$, and the adjustment of the probe center relative the surface is accomplished with small rotations ΔC. The details of the mathematical approach for measuring and correcting freeform surfaces are in Davies et al. [9] and Morgan [10].

4. Results

The mirror M3 blank was machined on a Makino A51 machine using NanoCAM4 to program the machine to mill the freeform shape. The mirror was mounted on the machine and measured. The error is shown in Figure 5(a), 51.1 µm peak to value (PV) and 10.5 µm rms, primarily defocus (mill radius) and decenter (mounting uncertainty). The surface was rough turned on the 650FG with an 0.2 mm carbide insert (Kennamettal VBGT110302HP Grade KC5410). The form error improved to Figure 5(d), 3.5 µm PV and 0.361 µm rms. The mirror was then finished with a 0.5153 mm radius diamond tool that had been calibrated by cutting a 15 nm rms test sphere over 45 degrees.

The initial measurement is shown in Figure 6(c). The freeform deviation has the correct character (see Figure 1). The error was dominated by defocus and primary spherical error as shown in Figure 6(d). The correction was subtracted from the prescription in NanoCAM4, and the surface was cut and measured again. Figure 7 shows the form error, now 420 nm PV and 80 nm rms, which met the tolerance in Table 1.

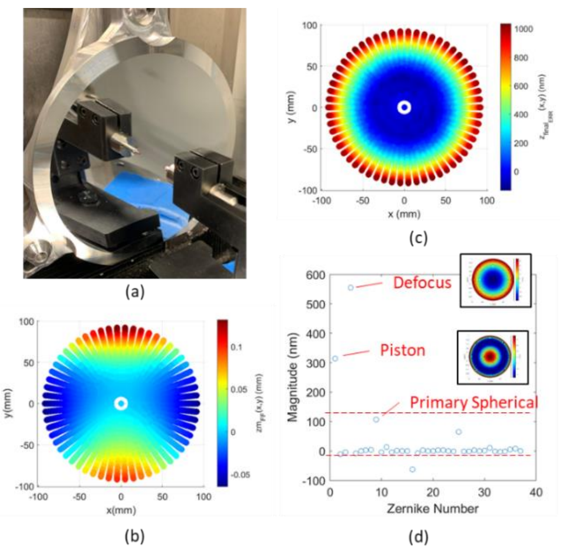

Figure 6. (a) Diamond turned surface, (b) measured freeform deviation, (c) measured error, (d) Zernike terms in fit of error - correction.

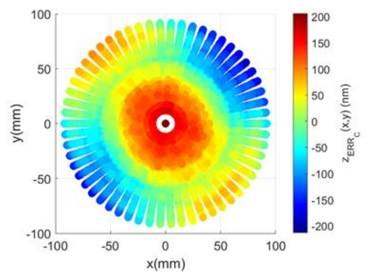

Figure 7. Final measured form error.

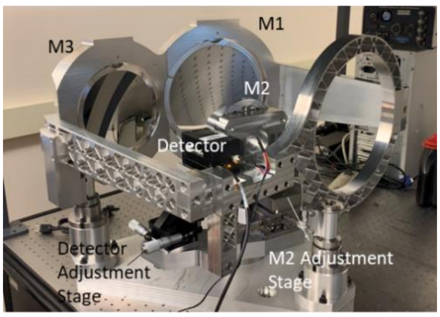

Figure 8. Assembled system.

Table 2. Estimate of achieved uncertainties from on-machine measurements on the Moore Nanotechnology 650FG and Makino A51.

Detector Limited Performance			
Motion	M1	M2	M3
X/Y Decenter [µm]	±125	Compensator	±125
Z Despace [µm]	±125	Compensator	±125
Tip/Tilt [µrad]	±115	±115	±115
Clocking [µrad]	±475	±475	±475
Irregularity (PV) [µm]	2 (1)	0.92 (0.46)	1.41 (0.71)
Power (Fringes*)	5	5	5

5. Summary

The final system has been constructed and is shown in Figure 8. The system was assembled and the assembly was measured inside the enclosure of a Makino A 51 machine. The final estimated uncertainties are given in Table 2 and are better than those required for detector-limited performance. The system is currently undergoing tuning and testing. This paper demonstrates the concurrent design and manufacturing of a freeform telescope with (expected) detector limited optical performance. Also, the ball-vee mounts, while not strictly kinematic mounts, are inexpensive to manufacture conventionally and meet the required assembly tolerances. When M2 has been adjusted for optimal performance, the position stage can be locked and the system is then effectively "snap together" similar in design to Horvath et al. [6]. Finally, the paper shows that by concurrent engineering to utilize freeform design degrees of freedom to make tolerances attainable by precision and ultraprecision machining, a relatively inexpensive and high-performance system can be manufactured and likely produced in large quantities.

Acknowledgements
We gratefully acknowledge the National Science Foundation (NSF) I/UCRC Center for Freeform Optics (IIP-1338877, IIP-1338898, IIP-1822049, and IIP-1822026).

References

[1] Thompson KP and Rolland JP 2012 Freeform optical surfaces: A revolution in imaging optical design *Opt. and Phot. News* **23(6)** 30

[2] Plummer WT, Baker JG and Van Tassel J Photographic optical systems with nonrotational aspheric surfaces 1999 *J. Appl. Opt*. **38** 3572-92

[3] Smilie PJ, Dutterer BS, Lineberger JL, Davies MA and Suleski TJ 2012 Design and characterization of an infrared Alvarez Lens, Optical Engineering *Opt. Eng.* **51(1)** 013006

[4] Rolland JP, Davies MA, Suleski TJ, Evans CJ, Bauer A, Lambropoulos K and Falaggis K 2021 Freeform optics for imaging *Optica* **8** 161-76.

[5] Bauer A, Schiesser EM and Rolland JP 2018 Starting geometry creation and design method for freeform optics *Nat. Commun.* **9** 1756.

[6] Horvath NW and Davies MA 2019 Concurrent engineering of a next generation freeform telescope: mechanical design and manufacture *Proc. SPIE* 10998 140-147

[7] Noste T, Evans CJ, Miller JA and Hopper LE 2019 Concurrent engineering of a next-generation freeform telescope: metrology and test *Proc. SPIE* 10998 148-156

[8] Horvath NW, Barron IW, Owen JD, Dutterer BS, Schiesser E, Bauer A, Rolland JP and Davies MA 2017 Optomechanical design and fabrication of a snap together freeform TMA telescope *Proc. ASPE 32nd Annual Meeting* 133-138

[9] Davis MA, Dutterer BS, Swagler S, Lawing E, Horvath N, Rolland JP, and Bauer A 2020 Optomechanical design and fabrication of a wide field of view 250-mm-aperture freeform imaging system *Adv. Maui Opt. and Space Surv. Tech. Conf. (AMOS)* – www.amostech.com

[10] Morgan CJ 2022 Form error compensation of freeform surfaces by Gaussian RBF interpolants *Proc. ASPE 37th Annual Meeting* to Appear